UNIVERSITY OF DELAWARE | College of Earth, Ocean, & Environment
SCHOOL OF MARINE SCIENCE & POLICY

Alexander R. Davies
Ph.D. Candidate and Research Assistant
700 Pilottown Road
Lewes, DE, USA 19956
ardavies@udel.edu

Dear Nature Geosciences Editor:

We wish to submit the manuscript entitled "The role of mesoscale energy in phytoplankton blooms and export in the Southern Ocean" for consideration as a research letter to Nature Geosciences.

This research letter highlights the role of mesoscale kinetic energy in bloom formation and organic carbon export in the energetic Drake Passage of the Southern Ocean. The data were collected using an APEX biofloat profiler sampling the full ocean water column every two days. To the authors' knowledge, this is the only biofloat in the world operating on a two-day profiling cycle. Consequently, the biofloat resolved the temporal development of a natural phytoplankton bloom and organic carbon export into the deep ocean (organic carbon sequestration). Our results suggest that low levels of mesoscale kinetic energy are a necessary condition for natural bloom formation while high levels of mesoscale kinetic energy appear to facilitate carbon export. We believe the high resolution observations of a bloom-export event within the context of mesoscale kinetic energy in Drake Passage will be of great interest to a broad range of readers.

Furthermore, artificial iron injection experiments over the last quarter of a century have reveal the Southern Ocean as an iron limited, high nitrate, low chlorophyll region. Our observations suggest that low kinetic energy is a precondition for bloom formation before the consideration of any other potentially limitation factors (micronutrients, macronutrients, grazing relaxation). We believe the low kinetic energy precondition has been overlooked, since most Southern Ocean iron injection experiments occurred in low kinetic energy environments. We believe this will also be of interest to readers, as the Southern Ocean has drawn considerable attention as a site for geoengineered atmospheric carbon drawdown.

The manuscript contains original research (never before published) and is not currently being considered for publication elsewhere. We wish to confirm that there are no known conflicts of interested associate with this publication and there has been no significant financial support of this study that could have influenced the outcome. The manuscript and been read and approved by all name authors.

We hope you find our manuscript suitable for publication and look forward to hearing from you.

Sincerely,

Alexander R. Davies

Inclusions:

In addition to this cover letter, the submission package contains seven files: .pdf version of the manuscript, .tex version of the manuscript, .pdf file containing supplementary figures, .mov supplementary movie, and three high resolution .png figure files (also embedded in the manuscript).

The role of mesoscale energy in phytoplankton blooms and export in the Southern Ocean

Alexander R. Davies*
School of Marine Science and Policy, College of Earth, Ocean & Environment, University of Delaware. 700 Pilottown Road, Lewes, DE 19958

Fabrice Veron
School of Marine Science and Policy, College of Earth, Ocean & Environment, University of Delaware. 112C Robinson Hall, Newark, DE 19716

Matthew J. Oliver
School of Marine Science and Policy, College of Earth, Ocean & Environment, University of Delaware. 700 Pilottown Road, Lewes, DE 19958

1 Introduction

Phytoplankton blooms and their export to the deep ocean are an important aspect of the carbon cycle. They act to draw down atmospheric carbon dioxide and package it as organic particulates that sink into the deep ocean, where carbon can be sequestered on millennial timescales[1]. Mechanisms for bloom formation include episodic nutrient supply[2], changes in turbulent mixing[3], and grazing relaxation[4]. The Southern Ocean is an iron limited[5, 6, 7], high nitrate, low chlorophyll region that has drawn considerable attention as a potential site for carbon drawdown through iron fertilization. However, there are no prolonged in-situ observations of the mechanisms driving naturally occurring blooms in this region. Here we show results from a biofloat that measured the development and export of a naturally occurring phytoplankton bloom in the Drake Passage. Our observations show low levels of mesoscale kinetic energy are necessary for bloom onset, which is confirmed by satellite observations. Post-bloom high mesoscale kinetic energy appears to facilitate bloom export to the deep ocean by changing the neutral density depths of aggregated cells. We suggest that low mesoscale kinetic energy is a precondition for bloom formation in the Drake Passage before other potentially limiting factors become significant.

2 Main Article

The Southern Ocean (SO) accounts for up to 25% of total ocean carbon uptake[8, 9]. Fluxes of atmospheric carbon dioxide (CO_2) across the air-sea interface occur on relatively short timescales; the turnover time for atmospheric CO_2 in the surface ocean is on the order of one to ten years. In contrast, the deep ocean can sequester carbon on the order of 100–1,000 years[1], making it an important carbon reservoir in the global carbon cycle. As Earth continues to warm[10], biological carbon uptake and sequestration (the "biological pump") in the SO is expected to enhance over the coming century [11].

Phytoplankton blooms occur in the well lit, nutrient rich regions of the surface ocean and convert CO_2 into organic carbon through oxygenic photosynthesis. If not respired by other trophic levels, phytoplankton blooms senesce, aggregate by cell-to-cell coalescence or in zooplankton fecal pellets, and sink into the deep ocean. In the deep ocean, phytoplankton are converted back to dissolved inorganic CO_2 through microbial decomposition or reach the ocean floor sediment where they are buried[1]. The standing stock of phytoplankton in the open SO is characterized by patchy, intense blooms within an otherwise unproductive[12, 13] and seasonally light limited[14] environment. Artificial fertilization experiments[7, 15, 16, 17] have shown iron to be the limiting micro-nutrient of phytoplankton blooms across the SO, which has become a potential site for augmenting the export of atmospheric CO_2 to the deep ocean through iron fertilization[18].

It is widely assumed that either seasonal or episodic mixing impacts the availability of both light and nutrients to phytoplankton. However there are no coincident in-situ observations that quantify the relationship between mesoscale kinetic energy and naturally occurring phytoplankton blooms in the SO. In this study, we investigate the mesoscale dynamics that influence the formation and senescence of naturally occurring phytoplankton blooms in the SO.

2.1 Biofloat Observations

An Autonomous Profiling EXplorer (APEX float) was deployed in Drake Passage on December 18, 2012 at 64.813° W and 59.870° S. The float collected data by profiling the water column from 2,000 dbar ($\sim$ 2,000 m) to the surface every two days between January 10 and June 4, 2013 (herein the observation period). Figure (1a) shows the float trajectory. The fast, two-day profiling cycle allowed the float to act as a near-Lagrangian tracer with respect to the surface ocean motion (see Methods, Supplementary Movie). This profiling frequency resolved mesoscale processes that have an energy peak around 10 days and 220 km in the Southern Ocean

The float is a "biofloat" because it measured vertical profiles of pressure, temperature, salinity, optical backscatter, colored dissolved organic matter (CDOM) fluorescence, and chlorophyll-a fluorescence. Figures (1b) and (1c) show observations of chlorophyll-a concentration ($[Chl]$, a proxy for phytoplankton abundance) and density (ρ) in the upper 500 m of the ocean (Supplementary Figures 1a-d shows temperature, salinity, particle backscatter and CDOM observations). To the authors' knowledge, these are the first reported observations from a biofloat operating on a two-day profiling cycle.

In Figure (1b), the phytoplankton biomass is most abundant in the upper 100 m where there is sufficient light for net growth. Because the biofloat nearly tracks the motion of the surface ocean (Supplementary Movie, Supplementary Figure 2), we observe the temporal development of a phytoplankton bloom beginning on day of year (DOY) 75. The bloom persists for $\sim$ 20 days (which is on the order of mesoscale processes[19]) with the peak bloom between DOY 85–89. After the naturally occurring bloom, organic carbon export is observed with peak export on DOY 105.

For our analysis, we chose $\rho = 1027.45\,\mathrm{kg\,m^{-3}}$ as the characteristic isopycnal for the upper ocean, rather than the mixed layer depth (MLD). The depth of this isopyncal (z_c) is highly correlated with the depths of surrounding isopycnals and tracks the deepest extent of the surface chlorophyll layer (Figure 1b). This makes z_c a reasonable depth bound for depth integrating chlorophyll concentrations (see Methods).

2.2 Natural Bloom Sequence

The development of a phytoplankton bloom requires phytoplankton growth to outweigh losses due to respiration, sinking, or grazing. This occurs by increasing access to limiting nutrients[2], relaxing potential losses like grazing[4], or changing residence time in the euphotic layer on seasonal[20] or turbulent[3] scales. Residence time in the euphotic layer has been approximated by the MLD[4, 20], however parameterizing upper ocean dynamics with the MLD may overlook critical surface ocean mixing processes that facilitate bloom formation[3]. Here we examine the role of mesoscale ocean dynamics in naturally occurring phytoplankton bloom formation in the SO.

At low mesoscale kinetic energy, stratification and the vertical structure of the ocean is ordered by hydrostatic equilibrium. However baroclinic instabilities that change the vertical structure of the ocean can occur at high mesoscale kinetic energies. Here we consider five-day averaged kinetic energy (KE) in the upper 30 m of the water column. The KE was computed using NOAA OSCAR currents and estimated at the float locations (see Methods). NOAA OSCAR currents resolve mesoscale dynamics (spatial processes on the order of 100 km and temporal processes on the order of 10 days in the SO[19]) resulting from geostrophic motion

caused by sea surface height anomalies and ageostrophic motion caused by wind-driven circulation and temperature gradients [21].

Figure (2a) is the temporal progression of column integrated chlorophyll-a concentration above z_c ($[Chl]|_c$) with respect to KE over the bloom-export period. Figure (2b) shows vertical $[Chl]$ profiles at key times during the bloom and export period. The progression begins on DOY 73 with moderate KE ($475\,\mathrm{cm\,s^{-2}}$) and low $[Chl]|_c$ ($136\,\mathrm{mg\,m^{-2}}$). As the bloom grew, KE decreased by 77% to $109\,\mathrm{cm\,s^{-2}}$ on DOY 85, while $[Chl]|_c$ more than doubled to $359\,\mathrm{mg\,m^{-2}}$. The MLD and z_c appear unchanged by the KE below $400\,\mathrm{cm^2 s^{-2}}$ indicating that the vertical structure of the water column was not sensitive to low KE (Figure 2c). We interpret this as a mesoscale analog to the formation of blooms during reduced turbulent mixing[3].

During peak bloom (DOY 85–89), the $[Chl]|_c$ in each profile was greater than $350\,\mathrm{mg\,m^{-2}}$. For comparison, the average $[Chl]|_c$ during the observational period was $147\,\mathrm{mg\,m^{-2}}$ with a standard deviation of $\pm$ $69\,\mathrm{mg\,m^{-2}}$. The KE continued to decrease to $55\,\mathrm{cm^2\,s^{-2}}$ on DOY 89 with a well defined surface phytoplankton bloom (Figure 2b).

After the peak bloom, $[Chl]|_c$ decreased by 42% between DOY 89–93 while KE remained below $62\,\mathrm{cm^2\,s^{-2}}$. The vertical $[Chl]$ profiles appear to indicate the $[Chl]$ loss is uniform with depth in the surface ocean. Backscatter also reduced in a similar manner (Supplementary Figure 3), indicating that the change in $[Chl]|_c$ in Figure (2a) was not due to changes in intracellular pigment concentrations. Furthermore, Figure (1b) does not show organic carbon export during between DOY 89–93. Our interpretation is that the prolonged low KE allowed a grazing ecosystem to organize around the concentrated phytoplankton bloom which is a mesoscale analog to seasonal ecosystem re-coupling of grazing pressure[22].

2.3 Export Sequence

Our observations suggest that bloom development is predicated on increasing phytoplankton residence time in the euphotic layer due to low KE, however the mechanisms driving organic carbon export are different. Between DOY 93–105, the $[Chl]|_c$ remained fairly constant (Figure 2a) with a decrease of only 16%. The KE increased by over an order of magnitude from 62 to 1,045 $\mathrm{cm^2\,s^{-2}}$ and z_c deepened from 175 to 289 m indicating that increased KE was sufficiently strong to alter the vertical structure of the water column (Figures 2a,c). This suggests that the post-grazed phytoplankton bloom is being diluted as z_c deepens (Figure 2a,b).

Phytoplankton export to the deep ocean occurred from DOY 101–109 while the KE remained high and z_c continued to deepen. Deep $[Chl]$ spikes (Figure 1b) coincide with spikes in the particle backscatter coefficient (b_{bp}, Supplementary Figure 1c). This suggests that these $[Chl]$ features are associated with aggregated phytoplankton[23] that rapidly sink out of the surface ocean[24]. We estimated a sinking rate of $125\,\mathrm{m\,day^{-1}}$ (see Methods) between DOY 103–105 which is comparable with other particle flux studies[25].

Given that aggregated phytoplankton sink until reaching their neutral density points, the KE-driven deepening of z_c and other isopycnals played a role in deepening phytoplankton biomass. Therefore, under high KE cell aggregates of a particular density are deeper in the water column than expected under a lower KE regime (Figures 1b, 2b), thus priming the system for deep ocean particle export. During the export event, the MLD remained essentially unchanged (Figure 1c); therefore it appears that the KE-driven deepening of

isopycnals (and the neutral density points of cell aggregates) is more important than MLD for phytoplankton export.

2.4 Kinetic Energy and Bloom Relationship

Biofloat observations during the bloom-export period suggest low KE regimes lead to bloom formation. However, the analysis of all biofloat $[Chl]|_c$ measurements and KE during the observation period (Figure 3a) indicates low KE is a necessary, but not sufficient condition for bloom formation. Low levels of KE do not appear strong enough to impact the vertical structure of the water column (Figure 2c), allowing for increased residence time within the well-lit euphotic layer [3, 20]. However, blooms are not always present during low KE as other limiting factors still exist [5, 14].

The in-situ relationship between KE and bloom formation (Figure 3a) creates an expectation that satellite observations of phytoplankton blooms should be more probable during low KE regimes. To test this expectation, we examined coincident estimates of satellite observed chlorophyll-a concentration and OSCAR KE (see Methods) across the entire Drake Passage during the observational period (Figure 3b). We conclude that the relationship between mesoscale kinetic energy and bloom formation observed by the biofloat is characteristic of the entire Drake Passage. Our observations are opposite of what is expected in North Atlantic Gyre (and most sub-tropical systems) where higher levels of kinetic energy are required to mix limiting nutrients into the euphotic layer [26].

No blooms were observed in our in-situ observations (Figure 3a) or satellite analysis (Figure 3b) during high KE regimes, suggesting that residence time in the euphotic zone is the primary limiting factor for naturally occurring phytoplankton blooms. However, a recent study by Venables and Moore[27] concluded that light limitation does not constrain the annual standing stock of chlorophyll-a in the SO, rather iron is the primary limiting agent. Similarly, our biofloat observations show the MLD remained fairly constant during the observational period and did not correlate with $[Chl]$ (Supplimentary Figure 4). This suggests the MLD could be the wrong parameter for evaluating bloom formation. Furthermore, SO blooms have generally only been observed where stratification provides a favorable light regime, even when iron is naturally in excess[28]. While iron concentration are decidedly low across much of the SO [5, 6], our analysis suggests that low KE is a necessary precondition for bloom formation. Since successful iron addition experiments[7, 15, 16, 17, 18] occurred in low KE environments (Supplementary Table 1), it is possible that the general experimental design of iron addition occludes KE as a major controlling factor of phytoplankton bloom formation in the SO.

3 Methods

3.1 Biofloat and Surface Current Tracers

Our interpretation of the observed bloom-export sequence is predicated on the notion that the biofloat, profiling the water column every two days, acts as a near-Lagrangian tracer with respect to the surface ocean motion. The biofloat trajectory during the bloom-export period is compared with surface tracer trajectories computed using the NOAA OSCAR five-day averaged currents estimated at the biofloat locations (see below). The u and v current

components at the biofloat locations are used to project the likely trajectories over the course of two days. Supplementary Figure (2) shows that the biofloat acts as a near-Lagrangian tracer with respect to motion in the surface ocean.

3.2 Biofloat Data Analysis

The biofloat instrument payload included a SeaBird model 41 CTD and a WET Labs Combination Fluorometer-Scattering-CDOM Sensor. Measurements were made at discrete sampling depths during ascent to the surface. Below 1,000 dbar measurements were made every 100 dbar, between 1,000 and 500 dbar measurements were made every 50 dbar, and above 500 dbar measurements were made every 5 dbar for a high resolution sampling of the upper ocean. Pressure is converted to depth by assuming hydrostatic balance with a standard atmosphere of pressure at the ocean surface. Density is calculated following Gill[29].

Profiles of temperature, salinity, particle backscatter coefficient and colored dissolved organic matter are shown in Supplementary Figures (1a-d). One profile (DOY 71) was eliminated from the analysis because it exhibited unrealistic and noisy density inversions. This may be due to a temporary blockage in the conductivity cell on that profile.

3.3 Characteristic Isopycnal

We chose $\rho = 1027.45\,\mathrm{kg\,m^{-3}}$ as the characteristic isopycnal of the system because it tracked the bottom of the surface chlorophyll layer better than the mixed layer depth (MLD; taken as the depth of maximum $\partial\rho/\partial z$ in each smoothed vertical density profile). Chlorophyll concentrations in excess of $1\,\mathrm{mg\,m^{-3}}$ were consistently observed below the MLD. This is an expected result because MLD does not explicitly correspond to the neutral density of phytoplankton cells which determines their vertical location in the water column. Furthermore, we believe the characteristic isopycnal is highly correlated to other isopycnals and interlaces the relationship between mesoscale kinetic energy and vertical density structure. Neither the KE or depth of the characteristic isopycnal (z_c) are strongly correlated with MLD ($R^2 = 0.43$ and 0.39, respectively). When compared with temperature observations (Supplementary Figure 1a), the MLD appears to track the top of the Antarctic Winter Water[30].

3.4 Daily Averaged Mean Kinetic Energy

National Oceanic and Atmospheric Administration (NOAA) Ocean Surface Current Analysis–Real time (OSCAR) currents were computed by combining a quasi-steady geostrophic model (derived from altimetry) with wind-driven ageostrophic currents and thermal wind adjustments. The currents are depth averaged to 30 meters (see Bonjean *et al.*[21] for full model description). The 1/3°resolution, five-day averaged surface current product we used is available at http://www.oscar.noaa.gov/.

The data product comes as discrete, temporal blocks of five-day averaged currents . We further process the OSCAR currents by assuming each block only represents the daily, five-day averaged current field (u_{daily} and v_{daily}) on the centered date. We linearly interpolated the five-day averaged currents to each day of the year. The daily, five day averaged kinetic

energy at each grid point is

$$KE_{daily} = \frac{1}{2}\left(u^2_{daily} + v^2_{daily}\right). \quad (1)$$

KE_{daily} is bi-linearly interpolated spatially to locations on Earth (KE) using a sphere.

3.5 Five Day Composite Surface Chlorophyll Concentrations

Daily, 9 km level 3 Moderate Resolution Imaging Spectroradiometer (MODIS) Aqua satellite [Chl] data was downloaded from http://oceancolor. gsfc.nasa.gov between January 10 and June 4, 2013. The data was subset to the three spatial boxes in Supplementary Figure 5 that represent the greater Drake Passage. Five day surface chlorophyll-a composites were made corresponding to each of the five-day averaged NOAA OSCAR data blocks processed.

3.6 Sinking Rates

Sinking rates are determined by changes in the deepest extent of twenty evenly spaced iso-chlorophyll lines between 0.1 - 0.4 $\mathrm{mg\,m^{-3}}$. The vertical change (Δz) between two filtered profiles (Δt) gives the sinking rate. The twenty sinking rates are averaged for one estimate of vertical motion between two filtered profiles.

4 Acknowledgments

The research was generously funded by the Charles and Patricia Robertson Research Fund and Graduate Fellowship. A.R.D. would like to thank Dr. Pablo Huq, Dr. Robert Vaillancourt, and Dr. Mark Moline for constructive discussion. A.R.D. would like to thank Scott Davies for assistance with the Supplementary Movie. The authors would like to thank Dr. Dana Veron for manuscript review.

5 Author Contributions

A.R.D. and M.J.O. co-wrote the manuscript and carried out the biofloat experiment. A.R.D. carried out all data processing and analysis. F.V. contributed to the manuscript. All authors contributed intellectually to the findings and conclusions.

References

[1] Ciais, P., Sabine, C., Bala, G., Bopp, L., Brovkin, V., Canadell, J., Chhabra, A., DeFries, R., Galloway, J., Heimann, M., Jones, C., Le Qur, C., Myneni, R. B., Piao, S. & Thornton, P. Carbon and Other Biogeochemical Cycles. In: *Climate Change 2013: The Physical Science Basis. Contribution of Working Group I to the Fifth Assessment Report of the Intergovernmental Panel on Climate Change* [Stocker, T. F., Qin, D., Plantter, G.-K., Tignor, M., Allen, S. K., Boschung, J., Nauels, A., Xia, Y., Bex, V., & Midgley, P. M. (eds.)]. Cambridge, United Kingdom and New York, NY, USA. 530–531 (2013).

[2] Falkwoski, P. G., Ziemann, D., Kolber, Z., & Bienfang, P. Role of eddy pumping in enhancing primary production in the ocean *Nature*, **352**, 55–58 (1991).

[3] Taylor, J. R. & Ferrari, R. Shutdown of turbulent convection as a new criterion for the onset of spring phytoplankton blooms. *Limnology and Oceanography*, **56**, 2293–2307 (2011).

[4] Behrenfeld, M. Abandoning Sverdrup's Critical Depth Hypothesis on phytoplankton blooms. *Ecology*, **91**, 977–989 (2010).

[5] Martin, J. H. Glacial-interglacial CO_2 change: The Iron Hypothesis. *Paleoceanography*, **5**, 1–13 (1990).

[6] Martin J. H., Gordon R. M. & Fitzwater, S. E. Iron in Antarctic waters. *Nature*, **345**, 156–159 (1990).

[7] Boyd, P. W. *et al.* A mesoscale phytoplankton bloom in the polar Southern Ocean stimulated by iron fertilization. *Nature*, **407**, 695–702 (2000).

[8] Takahashi, T., *et al.* Global sea-air flux based on climatological surface ocean pCO_2 and seasonal biological and temperature effects. *Deep-Sea Research II*, **49**, 1601–1622 (2002).

[9] McNeil, B. I., Metzl N., Matear, R. J. & Corbiere, A. An empirical estimate of the Southern Ocean air-sea CO_2 flux. *Global Biogeochemical Cycles*, **21**, BG3011 (2007).

[10] IPCC. Summary for Policymakers. In: *Climate Change 2013: The Physical Basis. Contribution of Working Group i to the Fifth Assessment Report of the Intergovernmental Panel on Climate Change* [Stocker, T. F., Qin, D., Plantter, G.-K., Tignor, M., Allen, S. K., Boschung, J., Nauels, A., Xia, Y., Bex, V., & Midgley, P. M. (eds.)]. Cambridge University Press, Cambridge, United Kingdom and New York, NY, USA. (2013).

[11] Sarmiento, J. L., Hughes, T. M. C., Stouffer, R. J. & Manade, S. Simulated response of the ocean carbon cycle to anthropogenic climate warming. *Nature*, **393**, 245–249 (1998).

[12] Moore, J. K. & Abbott, M. R. Phytoplankton chlorophyll distributions and primary production in the Southern Ocean *Journal of Geophysical Research*, **105**, 28709–28722 (2000).

[13] Arrigo, K. R., van Dijken, G. L. & Bushinsky, S. Primary production in the Southern Ocean, 1997–2006. *Journal of Geophysical Research*, **113**, C08004 (2008).

[14] El-Sayed, S. Productivity of the Antarctic Waters–A Reappraisal. In: *Marine Phytoplankton and Productivity* [Holm-Hansen, O., Bolis, L. & Gilles, R. (eds.)]. Springer Berlin Heidelberg, Germany. 19–34 (1984).

[15] Gervais, F., Riebesell, U. & Gorbunov, M. Y. Changes in primary productivity and chlorophyll *a* in response to iron fertilization in the Southern Polar Frontal Zone. *Limnology and Oceanography*, **47**, 1324–1335 (2002).

[16] Coale, K. H., *et al.* Southern Ocean Iron Enrichment Experiment: Carbon Cycling in High- and Low-Si Waters. *Science*, **304**, 408–414 (2004).

[17] Hoffmann, L. J. Peeken, I., Lochte, K., Assmy, P. & Veldhuis, M. Different reactions to Southern Ocean phytoplankton size classes to iron fertilization. *Limnology and Oceanography*, **51**, 1217–1229 (2006).

[18] Smetacek, V., *et al.* Deep carbon export from a Southern Ocean iron-fertilized diatom bloom. *Nature*, **487**, 313–319 (2012).

[19] Daniault, N. & Menard, Y. Eddy Kinetic Energy Distribution in the Southern Ocean From Altimetry and FGGE Drifting Buoys. *Journal of Geophysical Research*, **90**, 11877–11889 (1985).

[20] Sverdrup, H. U. On conditions for the vernal blooming of phytoplankton. *Journal du Conseli International pour l'Exploration de la Mer*, **18**, 287–295 (1953).

[21] Bonjean, F. & Lagerloef, G. S. E. Diagnostic Model and Analysis of the Surface Currents n the Tropical Pacific Ocean. *Journal of Physical Oceanography* **32**, 2938–2954 (2002).

[22] Behrenfeld, M. J & Boss E. S. Resurrecting the Ecological Underpinnings of Ocean Plankton Blooms. *Annual Review of Marine Science* **6**, 167–194 (2014).

[23] Briggs, N., Perry, M. J., Cetinic, I., Lee, C., D'Asaro, E., Gray, A. M. & Rehm, E. *Deep-Sea Research II* **58**, 1031–1039 (2011).

[24] Turner, J. T. Zooplankton fecal pellets, marine snow and sinking phytoplankton blooms. *Aquatic Microbial Ecology* **27**, 57–102 (2002).

[25] Fischer, G. & Karakas, G. Sinking rates and ballast composition of particles in the Atlantic Ocean: implications for the organic carbon fluxes of the deep ocean. *Biogeosciences* **6**, 85–102 (2009).

[26] Oschlies, A. & Garcon,V. Eddy-induced enhancement of primary production in a model of the North Atlantic Ocean. *Nature*, **394**, 266–269 (1998).

[27] Venables, V. & Moore, M. C. Phytoplankton and light limitation in the Southern Ocean: Learning from high-nutrient, high-chlorophyll areas. *Journal of Geophysical Research: Oceans*, **115**, C02015 (2010).

[28] Mitchell, B. G., Brody, E. A., Holm-Hansen, O., McClain, C. & Bishop, J. Light limitation of phytoplankton biomass and macronutrient utilization in the Southern Ocean. *Limnology and Oceanography*, **36**, 1662–1677 (1991).

[29] Gill, A. E. Appendix 3: Properties of Seawater In: *Atmosphere–Ocean Dynamics*. Elsevier Science. 599-600 (1982).

[30] Toole, J. M. Sea Ice, Winter Convection, and Temperature Minimum in the Southern Ocean. *Journal of Geophysical Research*, **86**, 8037–8047 (1981).

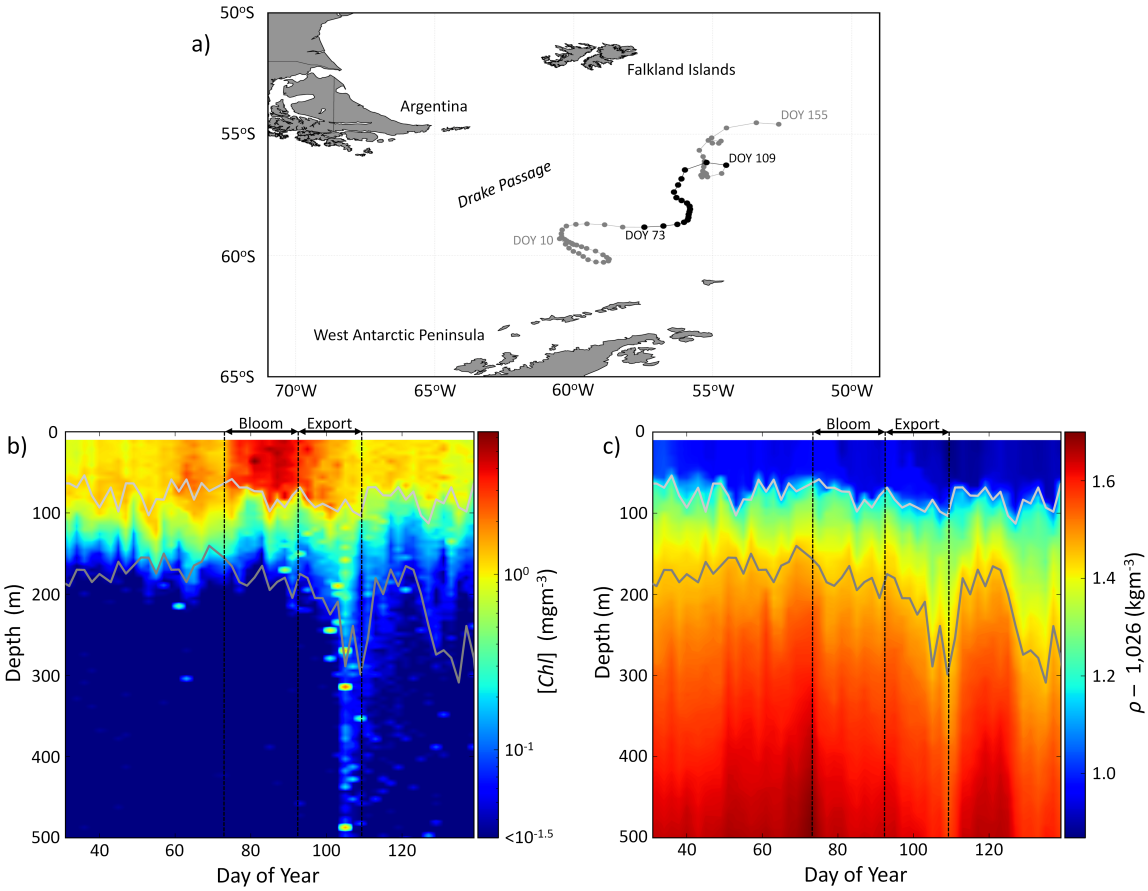

Figure 1: The a) biofloat trajectory, b) chlorophyll-*a*, and c) density observations. *a)* The biofloat profiled the water column from ∼2,000 m to the surface every-other day. The trajectory during the observational period (DOY 10–153) is plotted in gray with the bloom-export sequence (DOY 93–109) in black. *b,c)* Chlorophyll-*a* concentration ($[Chl]$) and density (ρ) observations from 500 m to surface, between DOY 31–139 are shown. The biofloat resolved mesoscale dynamics in the surface ocean, including the temporal progression of a naturally occurring phytoplankton bloom and export event (labeled). The mixed layer depth (light gray) remained fairly consistent during the observational period while the depth of the characteristic isopycnal (z_c, dark gray) deepended during export, indicating a change in the vertical structure of the water column. We chose $\rho = 1027.45\,\mathrm{kg\,m^{-3}}$ as the characteristic isopycnal for the upper ocean (see Methods).

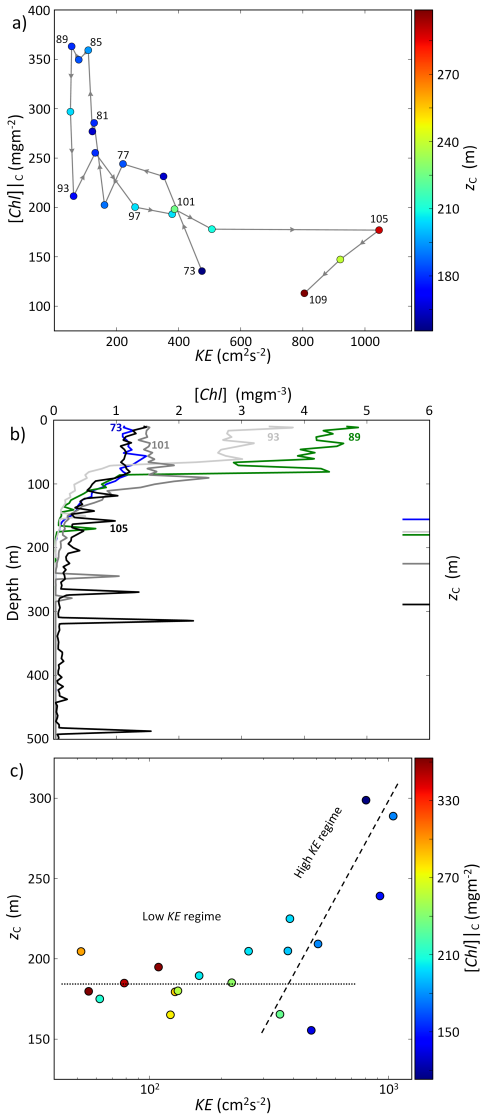

Figure 2: The development of a naturally occurring phytoplankton bloom and export event as function of kinetic energy and the depth of the characteristic isopycnal *a)* The temporal progression of the depth integrated chlorophyll-*a* concentration ($[Chl]|_c$) with respect to kinetic energy (KE). The sequence shows a developing bloom during low KE (DOY 73–89), phytoplankton loss likely due to ecosystem respiration and grazing (DOY 89–93), slow dilution corresponding to an increase in KE and deepening of the characteristic isopycnal (DOY 93–105), and organic carbon export into the deep ocean (DOY 101–109). *b)* Chlorophyll-*a* concentration ($[Chl]$) profiles show the peak bloom on DOY 89 is followed by peak carbon export between DOY 101–105. Horizontal marks on the right, vertical axis show the depth of the characteristic isopyncal (z_c) corresponding to each $[Chl]$ profile (coordinating colors). z_c deepend during peak export as *c)* KE appeared strong enough to impact the vertical structure of the water column (low KE seemingly does not impact the vertical structure).

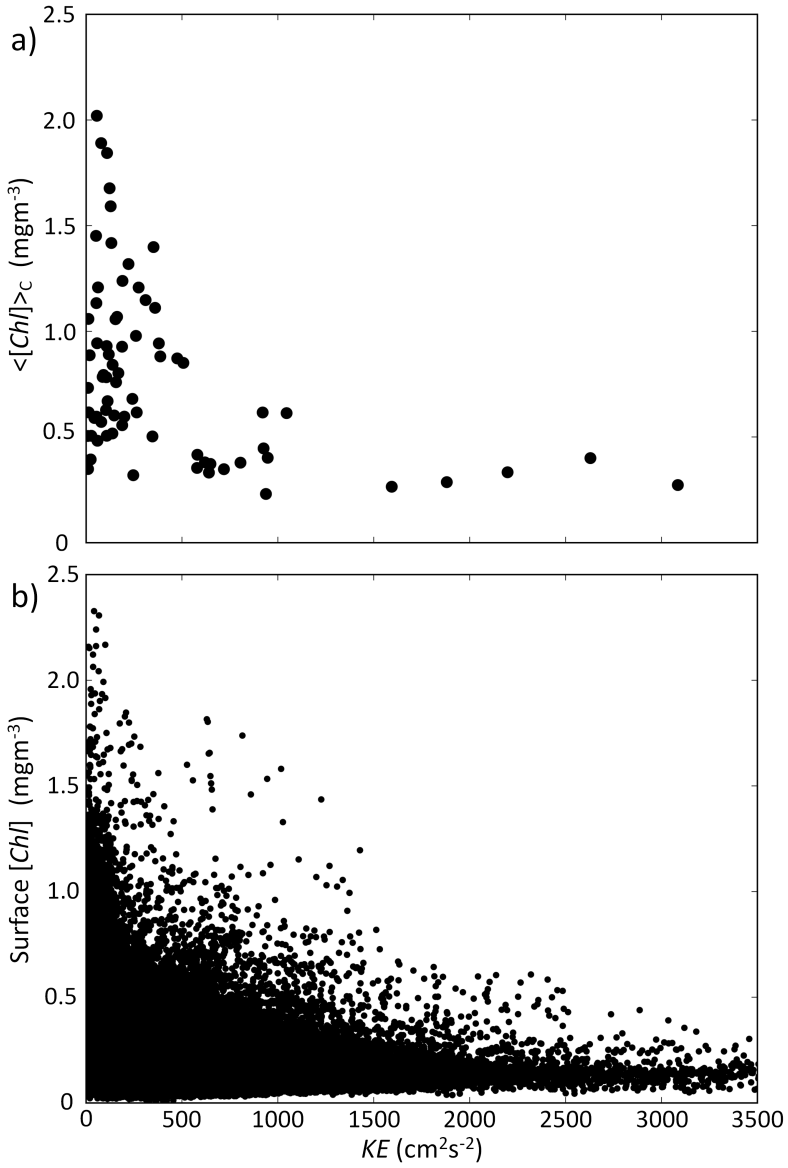

Figure 3: The relationship between kinetic energy and phytoplankton blooms. *a)* The depth averaged chlorophyll-a concentration above z_c observed from the biofloat ($<Chl>_c$) is plotted with respect to NOAA OSCAR kinetic energy (KE). Our in-situ observations suggest low KE is a necessary but not sufficient condition for phytoplankton blooms, while high KE limits blooms. *b)* To test applicability of these relationships across the Drake Passage, MODIS Aqua five-day composite surface chlorophyll-a concentrations (Surface [Chl]) are plotted with respect to KE. The KE and phytoplankton bloom relationship appears to hold across the broader Drake Passage during the observational period.

Supplementary Materials

The role of mesoscale energy in phytoplankton blooms and export in the Southern Ocean

Alexander R. Davies*
School of Marine Science and Policy, College of Earth, Ocean & Environment, University of Delaware. 700 Pilottown Road, Lewes, DE 19958

Fabrice Veron
School of Marine Science and Policy, College of Earth, Ocean & Environment, University of Delaware. 112C Robinson Hall, Newark, DE 19716

Matthew J. Oliver
School of Marine Science and Policy, College of Earth, Ocean & Environment, University of Delaware. 700 Pilottown Road, Lewes, DE 19958

Supplementary Movie

The supplementary movie shows the float locations (black dots) and NOAA OSCAR surface currents (gray arrows, see Methods). The gray arrows are scales to $1\,\mathrm{m\,s^{-1}}$ on the left hand side of the movie. The supplemental movie comes as a separate .mov file.

Supplementary Figure 1

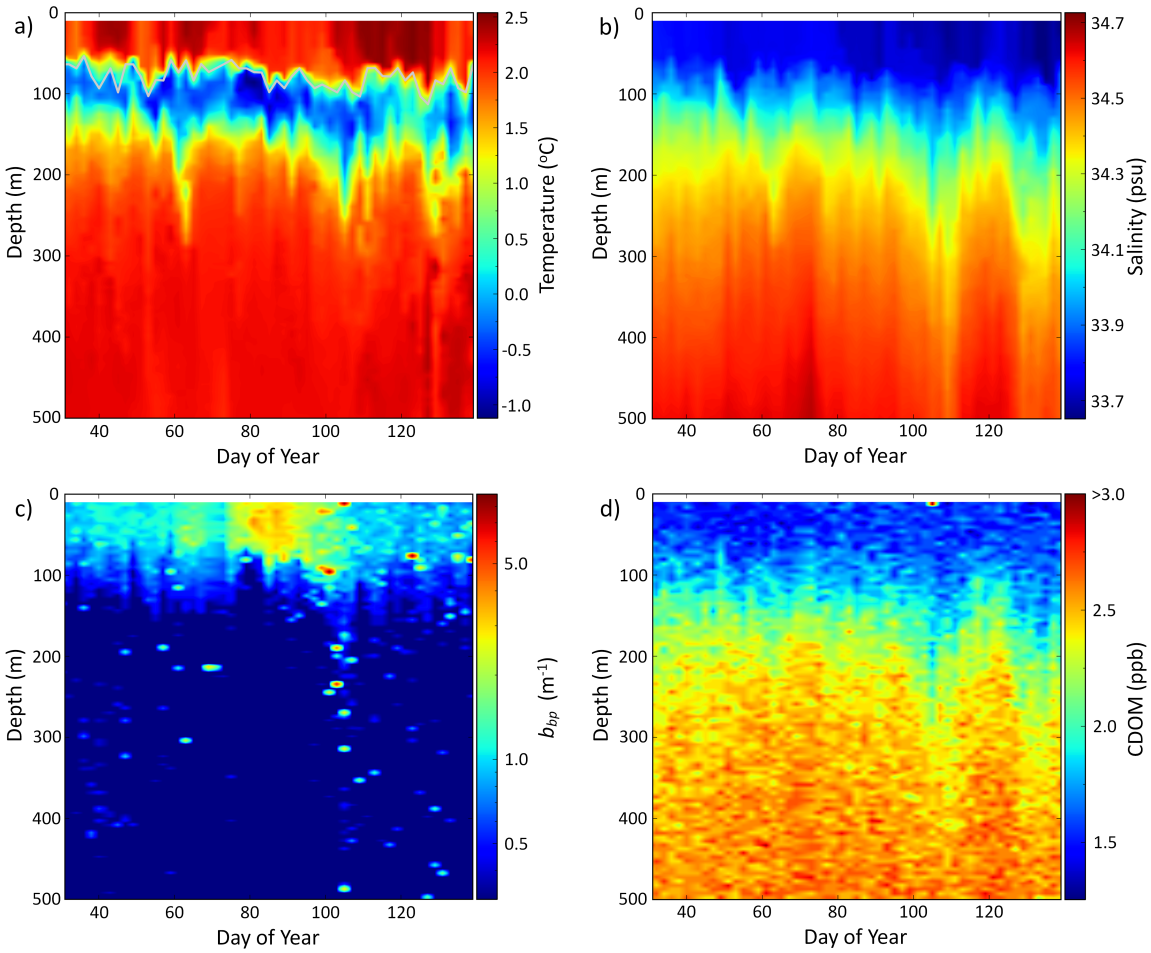

Figure 1: Biofloat *a)* temperature, *b)* salinity, *c)* back-scatter coefficient (b_{bp}), and *d)* colored dissolved organic matter (CDOM) observations. Observations from 500 m to the surface between DOY 31–139 are shown here. The mixed layer depth is the light gray line in *a)* and appears to track the top of the residual Antarctic Winter Water.

Supplementary Figure 2

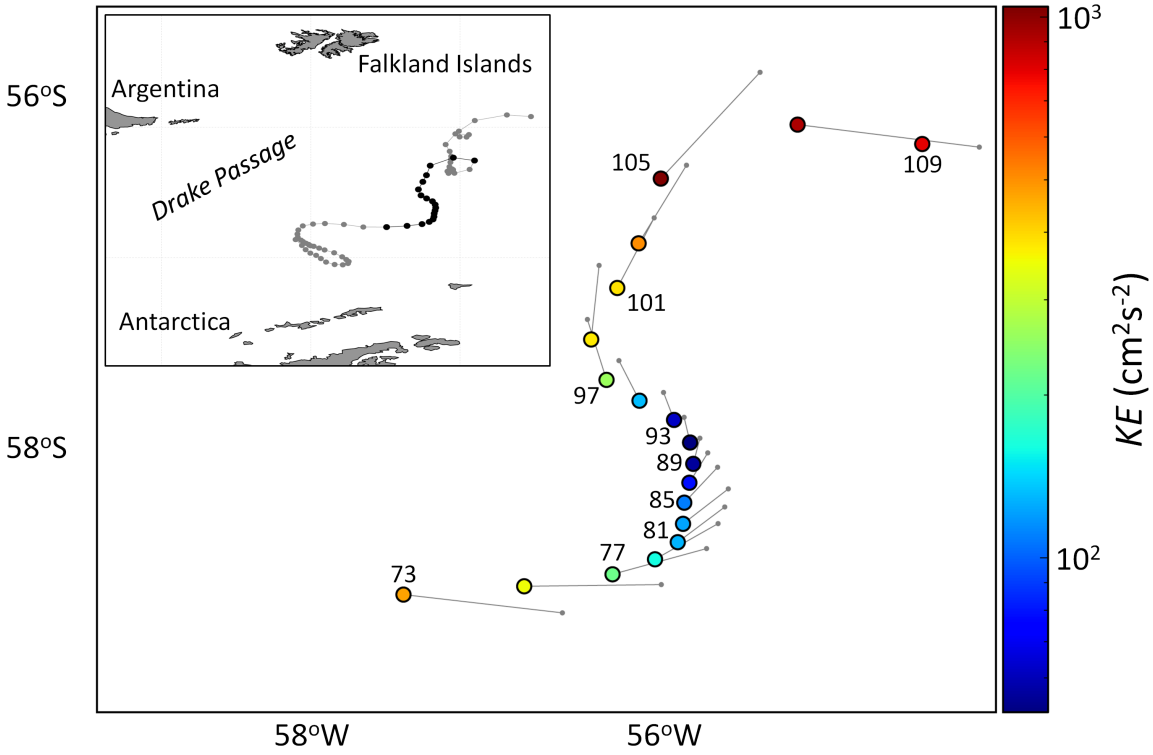

Figure 2: Biofloat and surface current tracer trajectories during the bloom-export event. The biofloat surfacing locations are shown and colored in accordance with the NOAA OSCAR kinetic energy (KE). Every-other DOY is labeled. The inset shows the entire trajectory during the observational period (gray) with the bloom-export event in black, and corresponding to the biofloat locations in the larger figure. The surface tracer trajectories were computed using the NOAA OSCAR five-day averaged currents estimated at the biofloat locations (see Methods). The u and v current components at the biofloat locations are used to project the likely trajectories over the course of two days. This allows for comparison with the two day sampling cycle of the biofloat. The surface tracer projection from each biofloat location are the gray lines and dots. Although not perfect, the biofloat acts as a near-Lagrangian tracer with respect to the surface ocean motion during the bloom-export period. To help ensure the float is not just randomly sampling the environment, we compared the normalized distance between the two-day tracer projections (gray dots) and corresponding biofloat locations with the depth of the characteristic isopycnal (z_c) and depth integrated chlorophyll-a concentrations ($[Chl|_c$). We found no significant correlations. The distance between the two-day tracer projections (gray dots) and the biofloat locations is normalized by the tracer projection distances. All distances were calculated on a sphere.

Supplementary Figure 3

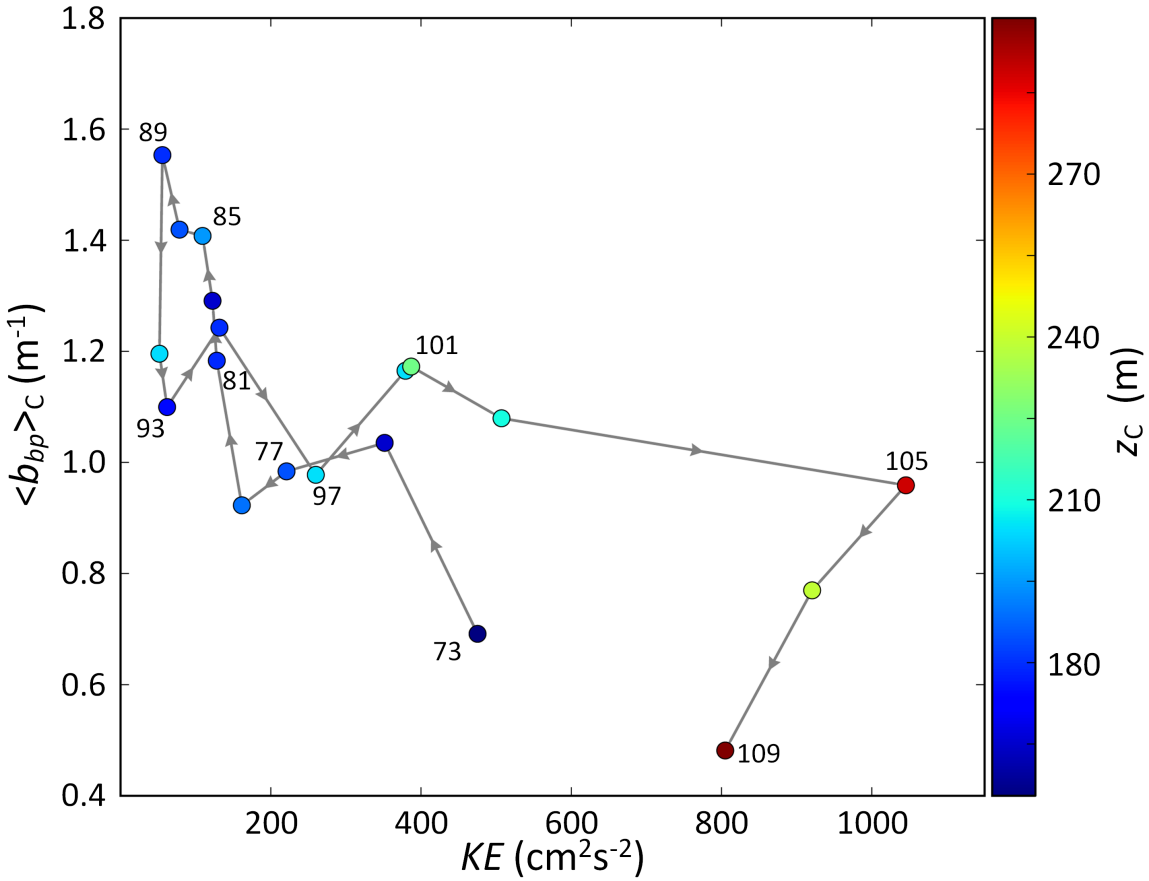

Figure 3: Particle backscatter during a naturally occurring phytoplankton bloom and export event with respect to kinetic energy *a)* The temporal progression of average particle backscattering above the characteristic isopycnal ($< b_{bpc}$) with respect to NOAA OSCAR kinetic energy (KE) during the bloom-export event. The observations are colored by the depth of the characteristic isopycnal (z_c) and every-other DOY is labeled. The sequence is similar to the progression of depth integrated chlorophyll-$a$concentration ($[Chl]|_c$) with respect to KE shown in Figure (2a), suggesting particle backscattering is primarily due to phytoplankton assemblages during this period. Most notably, a decrease in $< b_{bp} >_c$ between DOY 89 and 93 corresponds with a decrease in $[Chl]|_c$ in Figure (2a). This indicates the decrease in $Chl]|_c$ was not due to changes in intracellular pigment concentrations, rather a loss of phytoplankton biomass.

Supplementary Figure 4

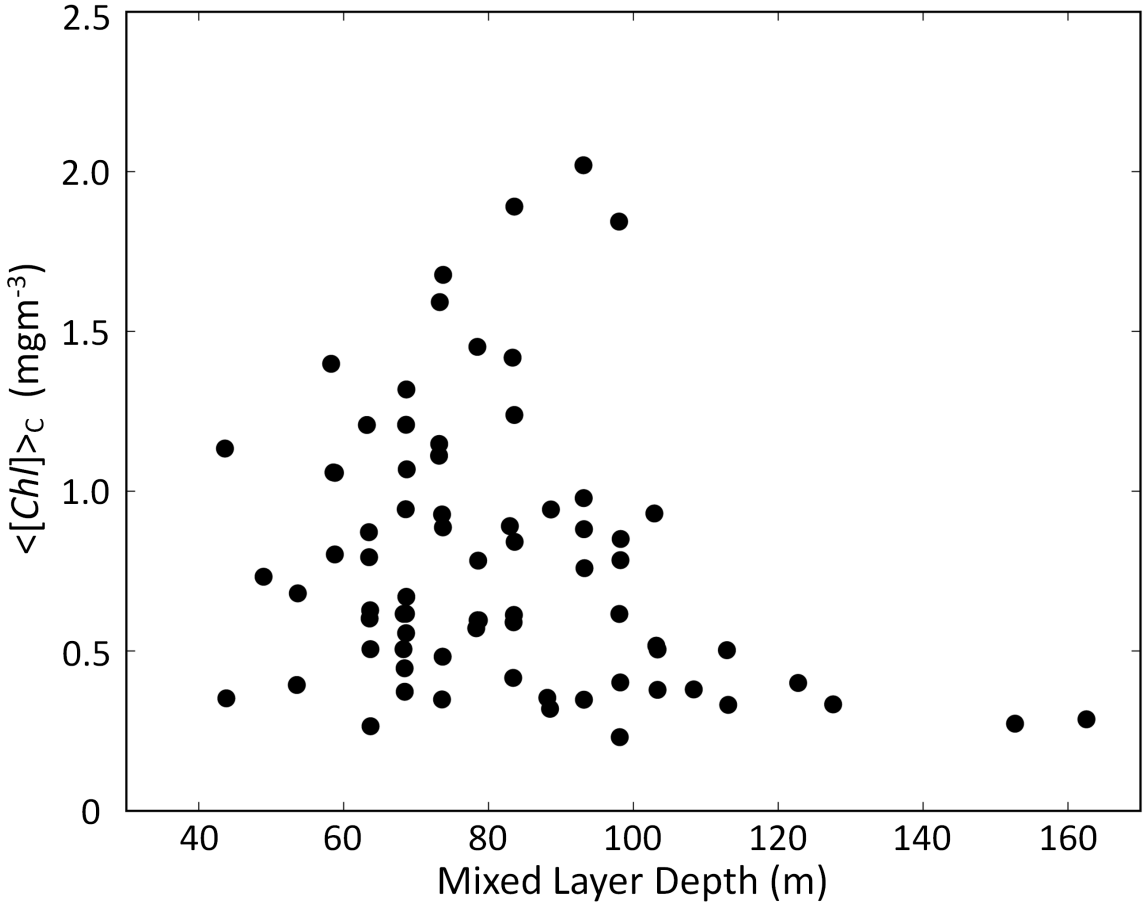

Figure 4: The relationship between mixed layer depth and phytoplankton blooms. The depth averaged chlorophyll-a concentration observed from the biofloat ($<[Chl]>_c$) is plotted with respect to the mixed layer depth. While low mesoscale kinetic energy appears to be a a necessary precondition for naturally occuring phytoplankton blooms and high mesoscale kinetic energy limits blooms (Figure 3), no clear relationship was observed with respect to the mixed layer depth. The data were measured by the biofloat.

Supplementary Figure 5

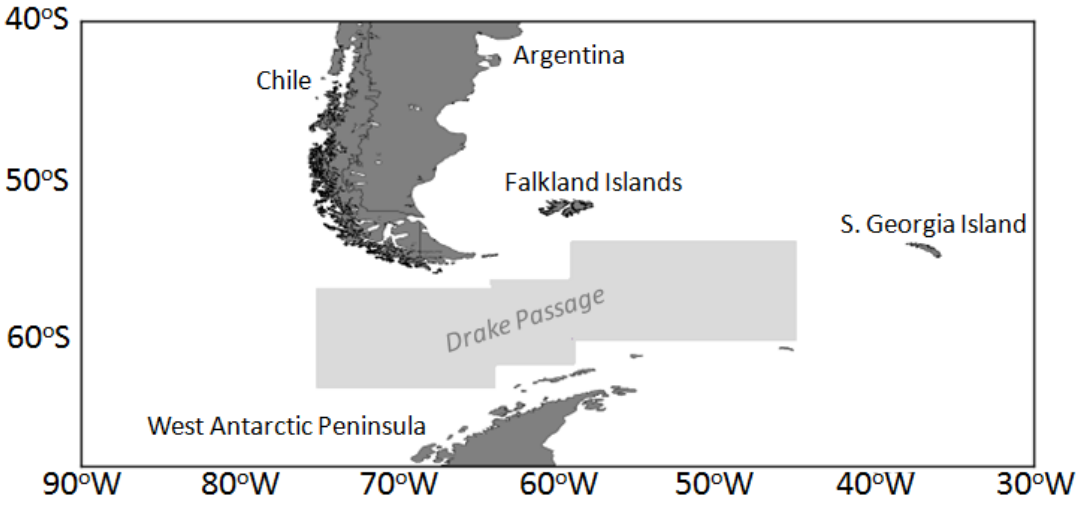

Figure 5: Comparison region (gray) for 9km, level 3 MODIS Aqua satellite chlorophyll-*a* concentrations and NOAA OSCAR kinetic energy observations (See Methods).

Supplementary Table 1

Study	Latitude	Longitude	Estimated *KE* range (cm^2s^{-2})	Notes
SOIREE	61.0° S	220.0° E	N/A	The site was chosen in-part due to "low eddy activity" and "low horizontal shear."
EisenEx	48.0° S	21.0° E	14.1–108.2	The iron injection was inside a mesoscale eddy to ensure "stable hydrographic conditions."
SoFEX South	66.5° S	188.2° E	17.3–33.7	A coherent patch was present throughout the experiment and slowly grew from 225 km^2 to 2,100 km^2.
SoFEX North	56.2° S	188.0° E	57.8–462.3	Strong horizontal shear stretched the patch into an "elongated filament" 7 km wide by 340 km long.
EIFEX	50.0° S	2.0° E	8.9–578.3	The iron injection was inside an eddy to ensure a "relatively stable water mass." Iron injections were on experiment days 0 and 15. The initial iron injection nearly doubled the observed chlorophyll-*a* concentration inside the eddy. However, the day 15 injection was followed by a plateau or slight dip in the observed chlorophyll-*a* concentration which is at time when we estimate the *KE* peaked ($\sim$ experiment day 20).

Table 1: Estimated mesoscale kinetic energy during iron fertilization experiments in the Southern Ocean. The five iron fertilization experiments in the Southern Ocean are SOIREE[1], EisenEx[2], SoFEX South and North[3], and EIFEX[4]. The NOAA OSCAR *KE* (See Methods) is estimated at the listed latitude and longitude locations listed over the duration of each experiment. The *KE* was not available at the SOIREE study location. Supplementary notes about the general *KE* conditions or experiment are also listed.

References

[1] Boyd, P. W. *et al.* A mesoscale phytoplankton bloom in the polar Southern Ocean stimulated by iron fertilization. *Nature*, **407**, 695–702 (2000).

[2] Gervais, F., Riebesell, U. & Gorbunov, M. Y. Changes in primary productivity and chlorophyll *a* in response to iron fertilization in the Southern Polar Frontal Zone. *Limnology and Oceanography*, **47**, 1324–1335 (2002).

[3] Coale, K. H., *et al.* Southern Ocean Iron Enrichment Experiment: Carbon Cycling in High- and Low-Si Waters. *Science*, **304**, 408–414 (2004).

[4] Hoffmann, L. J. Peeken, I., Lochte, K., Assmy, P. & Veldhuis, M. Different reactions to Southern Ocean phytoplankton size classes to iron fertilization. *Limnology and Oceanography*, **51**, 1217–1229 (2006).

Note: These citations are also cited in the main article.